Synthesis and Gelation of DOPA-Modified Poly(ethylene glycol) Hydrogels

Bruce P. Lee, Jeffrey L. Dalsin, and Phillip B. Messersmith*

Department of Biomedical Engineering, Northwestern University, 2145 North Sheridan Road, Evanston, Illinois 60208

Received April 3, 2002; Revised Manuscript Received May 23, 2002

3,4-Dihydroxyphenylalanine (DOPA) residues are known for their ability to impart adhesive and curing properties to mussel adhesive proteins. In this paper, we report the preparation of linear and branched DOPA-modified poly(ethylene glycol)s (PEG-DOPAs) containing one to four DOPA endgroups. Gel permeation chromatography−multiple-angle laser light scattering analysis of methoxy-PEG-DOPA in the presence of oxidizing reagents (sodium periodate, horseradish peroxidase, and mushroom tyrosinase) revealed the formation of oligomers of methoxy-PEG-DOPA, presumably resulting from oxidative polymerization of DOPA endgroups. In the case of PEG-DOPAs containing two or more DOPA endgroups, oxidative polymerization resulted in polymer network formation and rapid gelation. The amount of time required for gelation of aqueous PEG-DOPA solutions was found to be as little as 1 min and was dependent on the polymer architecture as well as the type and concentration of oxidizing reagent used. Analysis of reaction mixtures by UV−vis spectroscopy allowed the identification of reaction intermediates and the elucidation of reaction pathways. On the basis of the observed reaction intermediates, oxidation of the catechol side chain of DOPA resulted in the formation of highly reactive DOPA-quinone, which further reacted to form cross-linked products via one of several pathways, depending on the presence or absence of N-terminal protecting groups on the PEG-DOPA. *N*-Boc protected PEG-DOPA cross-linked via phenol coupling and quinone methide tanning pathways, whereas PEG-DOPA containing a free amino group cross-linked via a pathway that resembled melanogenesis. Similar differences were observed for the rate of gel formation as well as the molecular weight between cross-links ($\bar{M}_c$), calculated using equilibrium swelling and the Flory−Rehner equation.

Introduction

Marine and freshwater mussels secrete proteinaceous adhesive materials for adherence to the substrates upon which they reside.[1] The protein adhesives, called mussel adhesive proteins (MAPs), are capable of mediating the firm attachment of the organisms to a wide variety of objects, such as rocks, metal ship hulls, and wood structures. One of the defining characteristics of MAPs is the presence of L-3,4-dihydroxyphenylalanine (DOPA), an amino acid that is formed by posttranslational modification of tyrosine.[2] Recent evidence suggests that DOPA is primarily responsible for the exceptional adhesive characteristics of MAPs.[3,4] The adhesive properties of DOPA have long been speculated as being due primarily to direct interactions between the catechol side chains of DOPA and the surfaces to which they are adsorbed. Recently, Ooka and Garrell[3] used spectroscopic methods to demonstrate that adsorption of DOPA-containing peptides to gold surfaces is mediated by the direct coordination of surface metal atoms by catechol oxygens of the DOPA residues, which become deprotonated upon adsorption to the gold surface.

MAPs are initially secreted as fluids that undergo an in situ hardening reaction, and DOPA residues are also believed to participate in the intermolecular cross-linking reactions that lead to the formation of a solid adhesive plaque.[1] Although the cross-linking reactions are not fully understood, evidence suggests that oxidation of DOPA to DOPA-quinone or DOPA-semiquinone by catecholoxidase enzyme (or by nonenzymatic means) can lead to cross-linking either with other DOPA residues by a radical mechanism or with an amine by a Michael addition mechanism.[1,5,6] Using low molecular weight DOPA model compounds and mass spectroscopy, Deming and co-workers[4] recently confirmed that oxidation of DOPA is likely to be the principal mechanism by which intermolecular cross-linking occurs, although experiments conducted by Yamamoto and co-workers suggested a role for lysyl oxidase induced cross-linking,[7] and bis- and tris-complexes of DOPA with multivalent metal ions present in the marine environment may also contribute to cross-linking of MAPs.[8]

In an effort to duplicate the adhesive characteristics of MAPs in synthetic polymers, several groups have investigated the synthesis of adhesive polymers by incorporation of DOPA into synthetic polymer backbones, side chains, or endgroups.[4,9−17] Yamamoto and co-workers have employed solution synthesis to prepare DOPA-containing polyamino acids, including poly(DOPA) and polypeptide polymers consisting of numerous repeats of DOPA-containing motifs

* To whom correspondence should be addressed. Phone: (847) 467-5273. Fax: (847) 491-4928. E-mail address: philm@northwestern.edu.

10.1021/bm025546n CCC: $22.00 © 2002 American Chemical Society
Published on Web 07/04/2002

from *Mytilus edulis*, *Aulacomya ater*, and the liver fluke *Fasciola hepatica*.[9−12] The polymers were found to be water soluble and capable of being cross-linked in the presence of tyrosinase enzyme. More recently, Yu and Deming reported the synthesis of DOPA-containing synthetic polypeptides by copolymerization of *N*-carboxyanhydride monomers of lysine and DOPA.[4,15] The water-soluble copolymers were found to form gels in the presence of oxidizing agents, such as mushroom tyrosinase, H_2O_2, $NaIO_4$, and O_2.

In our laboratory we are utilizing biomimetic strategies to develop adhesive polymers for medical applications.[18,19] Recently, we described the preparation of DOPA-containing block copolymers that exhibited enhanced mucoadhesivity as a result of DOPA incorporation.[17] Here, branched and linear forms of the biocompatible polymer poly(ethylene glycol) (PEG) have been modified with DOPA endgroups and the resulting polymers polymerized into hydrogels. UV−vis spectroscopy, molecular weight characterization, and swelling experiments were utilized to reveal details of the chemical cross-linking mechanism and the physical properties of the resulting hydrogels.

Experimental Section

Materials. 4-arm-PEG-amine (PEG-$(NH_2)_4$, $\bar{M}_w = 10\,000$) was purchased from SunBio, Inc. (Walnut Creek, CA), while linear PEG-bis-amine (PEG-$(NH_2)_2$, $\bar{M}_w = 3400$) and methoxy-PEG-amine (mPEG-NH_2, $\bar{M}_w = 5000$) were purchased from Shearwater Polymers, Inc. (Huntsville, AL). Sephadex LH-20 was obtained from Fluka (Milwaukee, WI). *N*-Boc-L-DOPA dicyclohexylammonium salt, sodium periodate ($NaIO_4$), mushroom tyrosinase (MT, EC 1.14.18.1), and horseradish peroxidase (HRP, EC 1.11.1.17) were acquired from Sigma Chemical Company (St. Louis, MO). Triethylamine (Et_3N), hydrogen peroxide (30 wt %, H_2O_2), sodium molybdate dihydrate, and sodium nitrite were purchased from Aldrich Chemical Co. (Milwaukee, WI). L-Dopa was purchased from Lancaster (Windham, NH). 1-Hydroxybenzotriazole (HOBt) was obtained from Novabiochem Corp. (La Jolla, CA), and *O*-(benzotriazol-1-yl)-*N*,*N*,*N*′,*N*′-tetramethyluronium hexafluorophosphate (HBTU) was acquired from Advanced ChemTech (Louisville, KY).

Synthesis of DOPA-Modified PEG. Linear and branched DOPA-modified PEGs containing up to four DOPA endgroups were synthesized using standard carbodiimide coupling chemistry as described below. The structures of the four DOPA-modified PEGs are shown in Figure 1.

Synthesis of PEG-(N-Boc-DOPA)$_4$, I. PEG-$(NH_2)_4$ (6.0 g, 0.60 mmol) was reacted with *N*-Boc-L-DOPA dicyclohexylammonium salt (4.8 mmol), HOBt (8.0 mmol), and Et_3N (8.0 mmol) in 60 mL of a 50:50 mixture of dichloromethane (DCM) and dimethylformamide (DMF). HBTU (4.8 mmol) in 30 mL of DCM was then added, and the coupling reaction was carried out under argon at room temperature for 1 h. The solution was successively washed with saturated sodium chloride solution, 5% $NaHCO_3$, diluted HCl solution, and distilled water. The crude product was concentrated under reduced pressure and purified by column chromatography on Sephadex LH-20 with methanol as the mobile phase. The product was further purified by precipitation in cold methanol three times, dried in a vacuum at room temperature, and stored under nitrogen at −20 °C. ^{1}H NMR (500 MHz, $CDCl_3$/TMS): δ 6.81−6.77 (m, 2H, $C_6HH_2(OH)_2-$), 6.6 (d, 1H, $C_6H_2H(OH)_2-$), 6.05 (br, s, 1H), 5.33 (br, s, 1H), 4.22 (br, s, 1H, $C_6H_3(OH)_2-CH_2-CH(N-)-C(O)N-$), 3.73−3.41 (m, PEO), 3.06 (m, 2H, PEO−CH_2−N−C(O)−), 2.73 (t, 2H, $C_6H_3(OH)_2-CH_2-CH-$), 1.44 (s, 9 H, $(CH_3)_3C-$). Gel permeation chromatography−multiple-angle laser light scattering (GPC−MALLS): $\bar{M}_w = 11\,900$, $\bar{M}_w/\bar{M}_n = 1.01$.

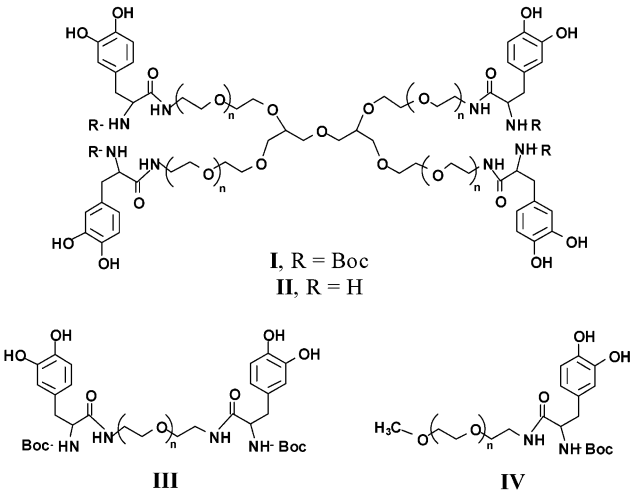

Figure 1. Chemical structures of DOPA-modified PEGs.

Synthesis of PEG-(DOPA)$_4$, II. **I** (3.0 g, 0.25 mmol) was dissolved in 15 mL of DCM at room temperature. TFA (15 mL) was added to the mixture to react for 30 min under argon. After evaporating the solvent in a rotary evaporator, the product was precipitated with cold methanol three times, dried in a vacuum at room temperature, and stored under nitrogen at −20 °C. ^{1}H NMR (500 MHz, D_2O): δ 6.79 (d, 1H, $C_6H_2H(OH)_2-$), 6.66 (s, 1H, $C_6H_2H(OH)_2-$), 6.59 (d, 1H, $C_6H_2H(OH)_2-$), 4.00 (t, 1H, $C_6H_3(OH)_2-CH_2-CH(N-)-C(O)N-$), 3.70−3.34 (M, PEO), 3.24 (m, 2H, PEG-CH_2−N−C(O)−), 3.01−2.88 (m, 2H, $C_6H_3(OH)_2-CH_2-CH(N-)-C(O)N-$). GPC−MALLS: $\bar{M}_w = 11\,400$, $\bar{M}_w/\bar{M}_n = 1.02$.

Synthesis of PEG-(N-Boc-DOPA)$_2$, III. PEG-$(NH_2)_2$ (5.0 g, 1.5 mmol), *N*-Boc-L-DOPA dicyclohexylammonium salt (5.9 mmol), HOBt (9.8 mmol), and Et_3N (9.8 mmol) were dissolved in 50 mL of a 50:50 mixture of DCM and DMF. HBTU (5.9 mmol) in 25 mL of DCM was then added, and the reaction was carried out under argon at room temperature for 30 min. Recovery and purification of the product were performed as described above for **I**. ^{1}H NMR (500 MHz, $CDCl_3$/TMS): δ 6.81−6.77 (m, 2H, $C_6HH_2(OH)_2$-), 6.59 (d, 1H, $C_6H_2H(OH)_2-$), 6.05 (br, s, 1H), 5.33 (br, s, 1H), 4.22 (br, s, 1H, $C_6H_3(OH)_2-CH_2-CH(N-)-C(O)N-$), 3.73−3.42 (M, PEO), 3.06 (m, 2H, PEO−CH_2−N−C(O)−), 2.74 (t, 2H, $C_6H_3(OH)_2-CH_2-CH(N-)-C(O)N-$), 1.44 (s, 9 H, $(CH_3)_3CO-$). GPC-MALLS: $\bar{M}_w = 4600$, $\bar{M}_w/\bar{M}_n = 1.02$.

Synthesis of methoxy-PEG-(N-Boc-DOPA), IV. mPEG-NH_2 (2.0 g, 0.40 mmol), *N*-Boc-L-DOPA dicyclohexylammonium salt (0.80 mmol), HOBt (1.3 mmol), and Et_3N (1.3 mmol) were dissolved in 20 mL of a 50:50 mixture of DCM and DMF. HBTU (0.80 mmol) in 10 mL of DCM was then added, and the reaction was carried out under argon at room

temperature for 30 min. Recovery and purification of the product were performed as described above for **I**. ^{1}H NMR (500 MHz, $CDCl_3$/TMS): δ 6.81−6.60 (m, 3H, $C_6H_3(OH)_2-$), 6.01 (br, s, 1H, OH−), 5.32 (br, s, 1H, OH−), 4.22 (br, s, 1H, $C_6H_3(OH)_2-CH_2-CH$(N−)−C(O)N−), 3.73−3.38 (m, PEO), 3.07 (m, 2H, PEO−CH_2−NH−C(O)−), 2.73 (t, 2H, $C_6H_3(OH)_2-CH_2-$CH(N−)−C(O)N−), 1.44 (s, 9 H, $(CH_3)_3C-$), 1.25 (s, 3 H, CH_3CH_2O-). GPC−MALLS: $\bar{M}_w$ = 6100, $\bar{M}_w/\bar{M}_n$ = 1.02.

DOPA Content Determination. The DOPA content of the DOPA-modified PEGs was determined by integration of relevant peaks in the ^{1}H NMR spectrum and by a colorimetric DOPA assay. In the NMR method, the DOPA content was measured by comparing the integral value of Boc methyl protons at δ = 1.44 to the PEG methylene protons at δ = 3.73−3.38. The DOPA assay was based on the previously described method of Waite and Benedict.[20] Briefly, PEG-DOPA aqueous solutions were treated with nitrite reagent (1.45 M sodium nitrite and 0.41 M sodium molybdate dihydrate) followed by the addition of excess NaOH solution. The absorbance (500 nm) of the mixture was recorded using a Hitachi U-2010 UV−vis spectrophotometer, within 2−4 min of NaOH addition. A standard curve was constructed using solutions of known DOPA concentration.

Formation of PEG-DOPA Hydrogels. To form PEG-DOPA hydrogels, sodium periodate ($NaIO_4$), horseradish peroxidase, and hydrogen peroxide (HRP/H_2O_2), or mushroom tyrosinase and oxygen (MT/O_2) were added to solutions of PEG-DOPA (200 mg/mL) in phosphate-buffered saline (PBS, pH 7.4). For gelation induced by MT, the PBS was sparged with air for 20 min prior to adding MT. Gelation time was qualitatively determined to be when the mixture ceased flowing, as measured by inversion of a vial containing the fluid.

Oscillatory Rheometry. Oscillatory rheometry was used to monitor the process of gelation and to determine the mechanical properties of the hydrogels. Cross-linking reagent was added to aqueous solution of PEG-DOPA, and the well-mixed solution was loaded onto a Bohlin VOR rheometer. The analysis was performed at a frequency of 0.1 Hz, a strain of 1%, and a 30 mm diameter cone and plate fixture with a cone angle of 2.5°.

Spectroscopic Evaluation of DOPA Oxidation. DOPA-modified PEG was dissolved in 10 mM PBS solution (bubbled with argon for HRP/H_2O_2 and $NaIO_4$ or air for MT experiments). After the oxidizing reagent was added, the time-dependent UV−vis spectra of the solution were monitored at wavelengths from 200 to 700 nm at a scan rate of 800 nm/min. All samples were initially blanked against PBS buffer and recorded at room temperature using a Hitachi U-2010 UV−vis spectrophotometer.

Molecular Weight Analysis. Molecular weights were determined by GPC−MALLS on a DAWN EOS (Wyatt Technology) using Shodex-OH Pak columns in an aqueous mobile phase (50 mM PBS, 0.1 M NaCl, 0.05% NaN_3; pH = 6.0) and a Optilab DSP (Wyatt Technology) refractive index detector. For molecular weight calculations, the experimentally determined dn/dc value of **IV** (0.136) was used.

Determination of Molecular Weight between Cross-Links. PEG-DOPA hydrogels were characterized by determination of the average molecular weight between cross-links ($\bar{M}_c$) as determined from equilibrium swelling data and application of the Flory−Rehner equation.[21,22] Disk-shaped hydrogels with a thickness of 1 mm were formed by addition of oxidizing reagents to aqueous PEG-DOPA solutions and gelation in a PTFE mold for 48 h. The gels were cut into disks of 4 mm diameter, and the mass of the relaxed gel (W_r) was determined. The gels were placed in excess distilled water and allowed to reach equilibrium before the mass of the swollen gels (W_s) was measured. The swollen gel was then dried in a vacuum at room temperature, and the mass of the dried gel (W_d) was determined. From the measured weight of the hydrogels, the densities of PEG (1.123 g/cm^3)[23] and water were used to find the volume of the gels in each state (V_r, V_s, and V_d in the relaxed, swollen, and dried state, respectively). The polymer volume fraction in the relaxed gel and the swollen gel, υ_r and υ_s, were calculated using the following two equations[24]

$$\upsilon_r = V_p/V_r \tag{1}$$

$$\upsilon_s = V_p/V_s \tag{2}$$

where V_p is the volume of PEG in the bulk hydrogel and is equal to V_d.

The equilibrium swelling data were used to calculate $\bar{M}_c$ using a modified Flory−Rehner equation that accounted for the formation of hydrogel in a solution[25,26]

$$\bar{M}_c = \frac{(1 - 2/\phi)\rho_p V_{H_2O} \upsilon_r^{2/3} \upsilon_s^{1/3}}{[\ln(1 - \upsilon_s) + \upsilon_s + \chi \upsilon_s^2]} \tag{3}$$

where ϕ is the cross-link functionality of the network junction, ρ_p is the density of PEG, V_{H_2O} is the molar volume of water (18.1 mol/cm^3), and χ is the Flory−Huggins parameter for PEG and water (0.462).[21]

ϕ was determined experimentally using the method of Gnanou et al.[27] Monofunctional **IV** was cross-linked by the addition of various oxidizing reagents and analyzed using GPC−MALLS 24 h after the initiation of oxidation. In general, GPC results showed two peaks, with one peak having molecular weight between a monomer and a dimer of **IV** while the molecular weight of the second peak corresponded to a multimer ($\bar{M}_{w,s}^{\mathbf{IV}} \geq 3\bar{M}_{w,o}^{\mathbf{IV}}$, where $\bar{M}_{w,s}^{\mathbf{IV}}$ and $\bar{M}_{w,o}^{\mathbf{IV}}$ are the molecular weights of cross-linked and unoxidized **IV**, respectively). Since three or more polymer chains are necessary to form a junction point, the average functionality of cross-linked **IV**, $\phi_{\mathbf{IV}}$, was estimated from

$$\phi_{\mathbf{IV}} = \bar{M}_{w,s}^{\mathbf{IV}}/\bar{M}_{w,o}^{\mathbf{IV}} \tag{4}$$

Values of $\phi_{\mathbf{IV}}$ were determined under conditions identical to those used in the formation of hydrogels from **I** and **III**. Since DOPA polymerization is the only source of junction formation for hydrogels formed from **III**, the value of $\phi_{\mathbf{IV}}$

Table 1. Molecular Weight and Coupling Efficiency of DOPA-Modified PEGs

composition	$\bar{M}_w$[a]	$\bar{M}_w/\bar{M}_n$[a]	% DOPA coupling efficiency	
			^{1}H NMR[b]	DOPA assay[c]
PEG-(*N*-Boc-DOPA)$_4$, **I**	11900	1.01	89.3	85.3 ± 2.0
PEG-(DOPA)$_4$, **II**	11400	1.02		80.9 ± 1.5
PEG-(*N*-Boc-DOPA)$_2$, **III**	4600	1.02	90.2	88.8 ± 6.5
MPEG-*N*-Boc-DOPA, **IV**	6100	1.02	96.9	86.3 ± 0.3

[a] Determined from aqueous GPC-MALLS. [b] Based on the Boc methyl protons at δ 1.44 and PEG methylene protons at δ 3.73−3.38 [c] $n = 3$.

determined by eq 4 was used in the calculation of $\bar{M}_c$ for these gels (i.e., $\phi_{III} \approx \phi_{IV}$).

Due to the branched architecture of **I**, the average functionality of hydrogels derived from **I** (ϕ_I) was estimated using the following equation

$$\phi_I = \frac{4P_{DOPA}\phi_{IV} + 4}{4P_{DOPA} + 1} \quad (5)$$

where P_{DOPA} is the probability that a DOPA end group forms a junction, which was determined by the extent of conversion from **IV** to multimers under identical conditions. Thus, P_{DOPA} was set equal to the weight fraction of the multimers of **IV**, w_s, which was determined from the following equation

$$w_s = \frac{m_s}{m_s + m_o} \quad (6)$$

where m_s and m_o are the masses of multimer and the monomer peaks, respectively.

Results and Discussion

DOPA-modified PEGs of different molecular weights and architectures were synthesized using standard peptide chemistry. NMR spectra (not shown) of these PEG-DOPA molecules revealed the presence of DOPA. The molecular weight and the DOPA coupling efficiency of these PEG-DOPA constructs are shown in Table 1. Typically, over 80% of the PEG end groups were functionalized with DOPA residues. All PEG-DOPA polymers were white solids that were freely soluble in water.

Formation of PEG-DOPA Hydrogels. Under oxidizing conditions, concentrated aqueous solutions of PEG-DOPA polymers **I**, **II**, and **III** formed rigid hydrogels in as little as 1 min, with gelation time dependent on PEG-DOPA architecture (linear vs branched) and type/concentration of oxidizing agent ($NaIO_4$, HRP/H_2O_2, MT/O_2). Under no conditions did polymer **IV** form a gel. Oscillatory rheology was used to monitor the process of gel formation. Mixtures of PEG-DOPA and cross-linking reagent were mixed and immediately loaded onto the testing platform in the fluid state. The dynamic storage modulus (G') of the polymeric fluid of **I** was recorded during periodate-induced curing as shown in Figure 2A. G' began to increase approximately 10 min after addition of periodate and continued to rise until it reached a maximum value of 13 kPa 8 h after initiation of the cross-linking reaction. At the conclusion of the rheometry experiment, frequency and strain sweep were performed on

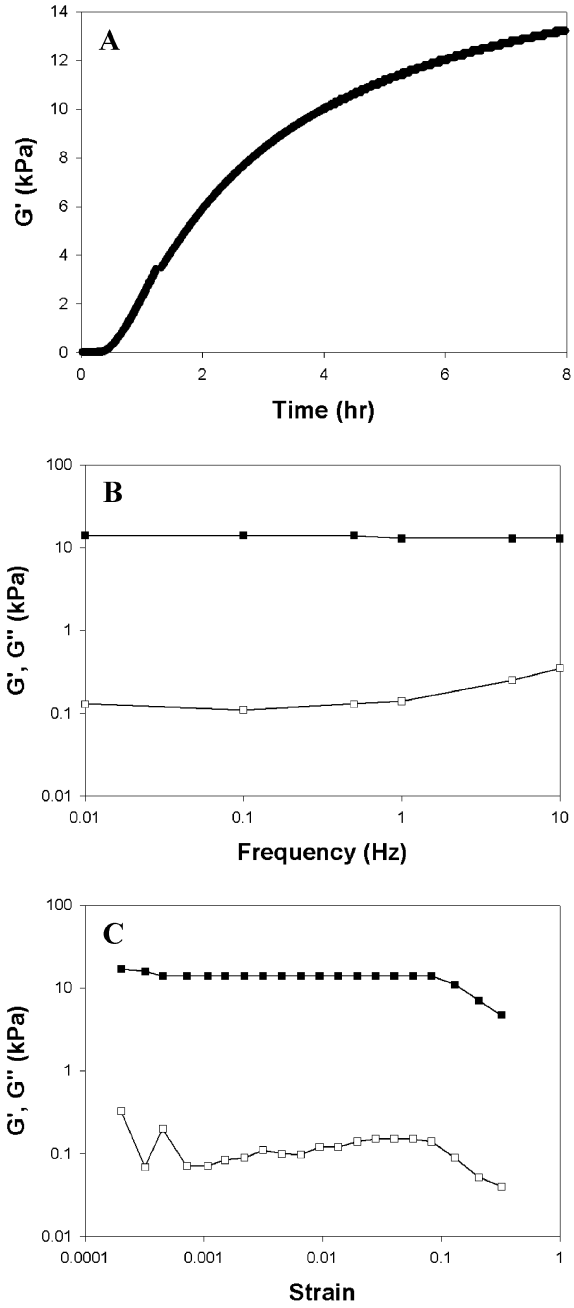

Figure 2. Rheological analysis of hydrogel formation from a 130 mg/mL solution of **I**: (A) dynamic storage modulus (G') as a function of time after addition of 75 mM $NaIO_4$ ($NaIO_4$:DOPA = 2.0); (B) strain sweep performed at 0.1 Hz; (C) frequency sweep performed at a strain of 0.006. In **B** and **C** the symbols denote G' (■) and G'' (□).

the cured gel (Figure 2B,C). G' was found to be both frequency and strain (<9%) independent, suggesting that the gelation process was complete.

Rheological analysis of the hydrogels formed from **II** and **III** revealed similar characteristics, although the gelation time was strongly dependent on the polymer, the type of oxidizing reagent, and its concentration (Figure 3). In the periodate-induced curing (Figure 3A), gelation time of Boc-protected polymers (**I** and **III**) showed a strong dependence on the $NaIO_4$ to DOPA molar ratio. Both **I** and **III** exhibited a minimum gelation time at approximately equimolar amounts of $NaIO_4$:DOPA. Under optimum conditions, gelation occurred in less 1 min for **I** and under 7 min for **III**. The

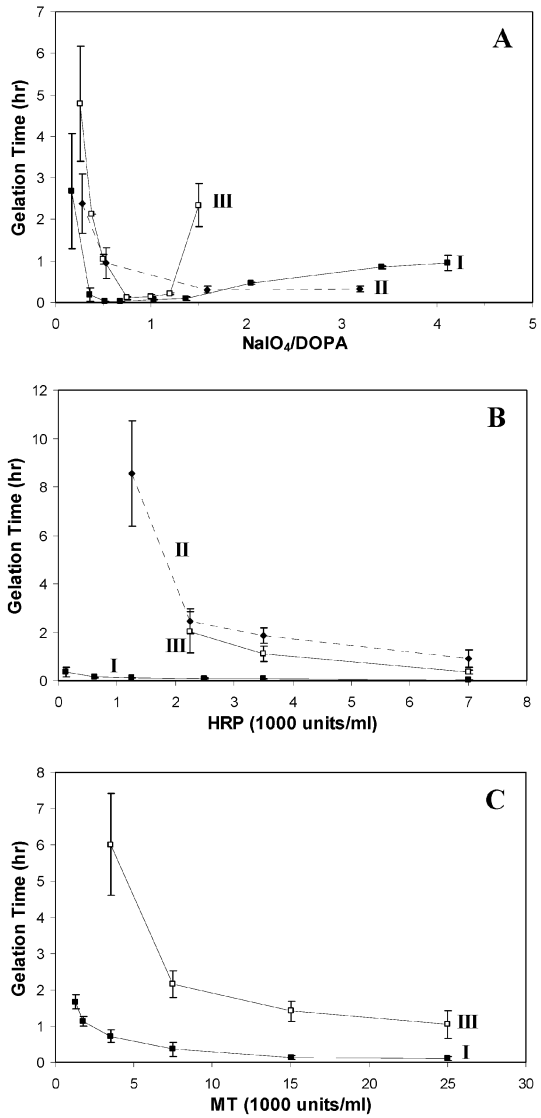

Figure 3. Gelation times of DOPA-modified PEG induced by addition of $NaIO_4$ (A), HRP and 0.24 mM H_2O_2 (B), and MT/O_2 (C) to 130 mg/mL solutions of PEG-DOPA in 10 mM PBS at pH 7.4. In (B), **III** did not gel at HRP concentration below 2000 units/mL. In (C), **II** incubated in 25 000 units/mL of MT took over 2 days to gel and no gelation was observed at lower MT concentrations. No gel formation was observed for **IV** using the concentrations of oxidizing reagents tested.

gelation time of deprotected **II** decreased exponentially with increasing periodate concentration. The minimum gelation time for **II** was around 18 min, which occurred at $NaIO_4$:DOPA = 3.2.

The gelation times of enzymatic cross-linking are shown in Figure 3B,C, respectively. For both HRP and MT, gelation time decreased exponentially with increasing enzyme concentration and **I** gelled faster than both **II** and **III**. At the highest HRP concentration tested (7000 units/mL), **I** gelled in 2 min as opposed to 20 and 90 min for **III** and **II**, respectively. At a MT concentration of 25 000 units/mL, **I** gelled in less than 6 min, **III** cured in just above an hour, and gelation of **II** was observed almost 2 days after the addition of the enzyme.

The gelation data suggest that PEG architecture, among other factors, played an important role in determining the gelation time. For the Boc-protected species, **I** cured much faster than **III** for the three cross-linking reagents utilized. The branch point in the architecture of **I** acts as a physical cross-link and facilitated the formation of networks. The fact that **III** was able to gel implies that oxidative DOPA cross-linking forms a physical junction point in which at least three DOPA residues were coupled together. Because of its monofunctionality, cross-linking of **IV** cannot lead to gelation, although it formed oligomers which were analyzed (Figure 6) to determine ϕ, the cross-link functionality of gels formed from **III** and **I**.

UV−vis. To understand the mechanisms behind the cross-linking of DOPA-modified PEG, reaction mixtures were monitored over time using UV−vis. By comparison of the observed UV−vis spectra obtained during the reaction to the known absorbance maxima of DOPA oxidation products,[28−30] the reaction pathways can be identified. Possible reaction pathways for oxidation of DOPA are shown in Scheme 1.[31,32]

***N*-Boc-Protected.** UV−vis spectra of the reaction of **I** are shown in Figure 4. In $NaIO_4$-mediated oxidation (Figure 4A), a peak at 392 nm typical of DOPA quinone[28] was observed immediately after the addition of $NaIO_4$. This peak was prominent during the initial stages of the reaction when the $NaIO_4$ concentration was greater than or equal to the DOPA concentration but decreased in intensity with time. At equimolar and substoichiometric concentrations of $NaIO_4$ (not shown), the 392 nm peak disappeared quickly (within 1 min of periodate addition) while at the same time a peak emerges with $\lambda_{max} = 330$ nm.

Rzepecki and Waite observed a similar concentration dependence for the periodate-mediated oxidation of *N*-acetyl-DOPA ethyl ester (NADEE).[33] The intensity and the decay rate of the quinone characteristic peak at 392 nm were observed to be dependent on the stoichiometric ratio of periodate to NADEE. Furthermore, at all periodate concentrations tested, emergence of α,β-dehydro derivative of NADEE (320 nm) occurred concurrently with the decay of the peak at 392 nm.[33] Upon oxidation of DOPA, the corresponding quinone tautomerized nonenzymatically via a quinone methide to α,β-dehydro-DOPA (Scheme 1, reactions B and C).[31,33] Thus, we conclude that oxidation of *N*-Boc-protected PEG-DOPA results in the formation of an α,β-dehydro product.

Formation of α,β-dehydro-DOPA has been suggested as a possible route for DOPA cross-link formation (Scheme 1, reaction D).[31,33] Both the quinone methide and the α,β-dehydro derivatives of DOPA are capable of further cross-linking reactions, which have been well characterized using *N*-acetyl-dopamine (NADA), a sclerotizing or cross-linking agent found in insect cuticles.[31] Dimers of NADA and its derivatives have been isolated by Andersen and colleagues.[34,35] Furthermore, quinone methide is capable of reacting with water, alcohol, thiols, acids, amines, and cellular components with appropriate reactive groups.[36] It is likely that *N*-Boc-DOPA-modified PEG underwent coupling reactions involving either DOPA quinone methide or α,β-dehydro DOPA as the oxidation intermediate similar to the cross-linking between *N*-acetyl-dopamine molecules.

Scheme 1. Oxidative Reactions and Possible Cross-Linking Pathways of DOPA and the Known UV−Vis Absorbance Maxima of Reaction Intermediates[a,28−32]

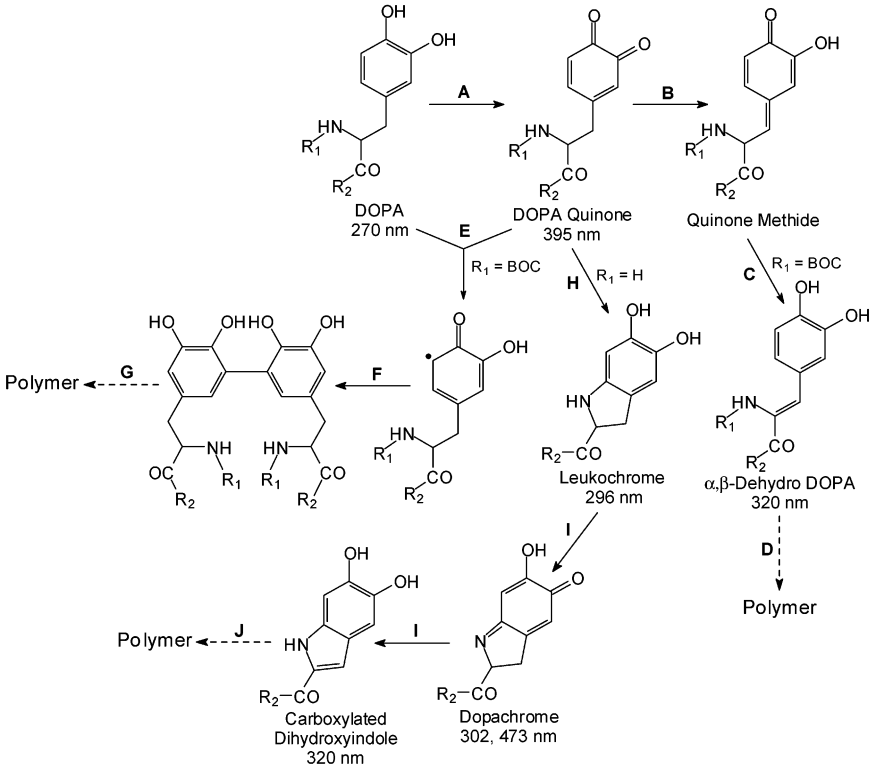

[a] Key: (A) Oxidation by catechol oxidase or other oxidizing reagents. (B) Tautomerization of DOPA quinone. (C) Release of α proton. (D) Cross-linking by a pathway similar to that occurring in insect cuticle sclerotization. (E) Aryloxy free radical generation. (F) Phenol coupling. (G) Further oxidation to form cross-linked polymer. (H) Internal cyclization with $R_1 = H$. (I) Rearrangement of cyclized DOPA derivatives. (J) Cross-linking by a pathway resembling that occurring in melanin formation. Dashed arrows indicate poorly understood pathways that lead to the formation of cross-linked polymers.

Oxidation of **I** with HRP/H_2O_2 (Figure 4B), resulted in an increase in intensity and a slight shift of the DOPA peak from 278 to 272 nm, the emergence of a peak at 415 nm, increase in the absorbance between 300 and 350 nm, and the formation of a broad peak at 484 nm. The peak at 415 nm is distinctive of HRP in the presence of H_2O_2.[37] Increase in the absorbance at 330 nm could suggest the formation of α,β-dehydro DOPA as observed in periodate-mediated oxidation, although no well-defined peak was observed. The peaks at 272 and 484 nm compared favorably to the spectrum of a dicatechol (λ_{max} = 268, 420 nm at pH 3 and λ_{max} = 274, 510 nm at pH 9) formed via phenol coupling of 4-methylcatechol.[38] Phenol coupling was suggested to occur through aryloxy radical formation (Scheme 1, reactions E and F), although dimers of phenol coupling products have not been isolated.[39] Interestingly, 5,5′-di(3,4-dihydroxyphenylalanine) (diDOPA) cross-link was recently detected by McDowell et al. using solid-state ^{13}C NMR analysis of byssal attachment plaques.[40]

Tyrosinase-induced oxidation of **I** was also studied in PBS solution saturated with air. Immediately after the addition of the enzyme, there was a significant increase in the absorbance intensity of the DOPA peak, which shifted slightly toward 272 nm after 24 h of incubation (Figure 4C). This peak along with the increase in the absorbance at wavelengths greater than 400 nm suggests the accumulation of phenol coupling products. A shoulder between 310 and 380 nm was also observed implying the formation of α,β-dehydro DOPA intermediates.

***N*-Boc-Deprotected.** Oxidation of **II** did not result in the same UV−vis spectra as its *N*-Boc-protected counterpart. Addition of $NaIO_4$ to aqueous solutions of **II** (Figure 5A) initially resulted in the formation of peaks with λ_{max} at 285, 299 nm, and a broad peak with λ_{max} = 463 nm. The peaks at 299 and 463 nm suggested the formation of dopachrome (λ_{max} = 302, 473 nm),[28] while the peak at 285 nm may be a combination of the characteristic peaks of leukochrome (λ_{max} = 296 nm),[28] dopachrome, and unreacted DOPA. The broad peak at 463 nm decayed over time as dopachrome underwent further reaction to form 5,6-dihydroxyindole-2-carboxylic acid (λ_{max} = 320 nm).[30] Similarly, in MT/O_2 oxidation (Figure 5B), dopachrome peaks (295, 458 nm) was observed initially but decayed with time as dopachrome further transformed to the DOPA indole derivative with λ_{max} = 324 nm. Dopachrome was initially observed for the HRP/H_2O_2-mediated reaction (Figure 5C), and there was a continuous increase in the intensity of the peak at 320 nm, suggesting the formation of dihydroxyindole derivative of DOPA.

Collectively, the UV−vis data suggest that PEG-DOPA conjugates with a free *N*-terminus oxidized to form cyclized products almost immediately after the initiation of a cross-linking reaction, with leukochrome and dopachrome being the first reaction intermediates observed. It is likely that DOPA was first oxidized to form DOPA quinone (Scheme 1, reaction A), which rapidly transformed into leukochrome by intramolecular cyclization (Scheme 1, reaction H). Although DOPA quinone was not observed in the UV−vis spectra, rapid scan experiments have shown the rapid

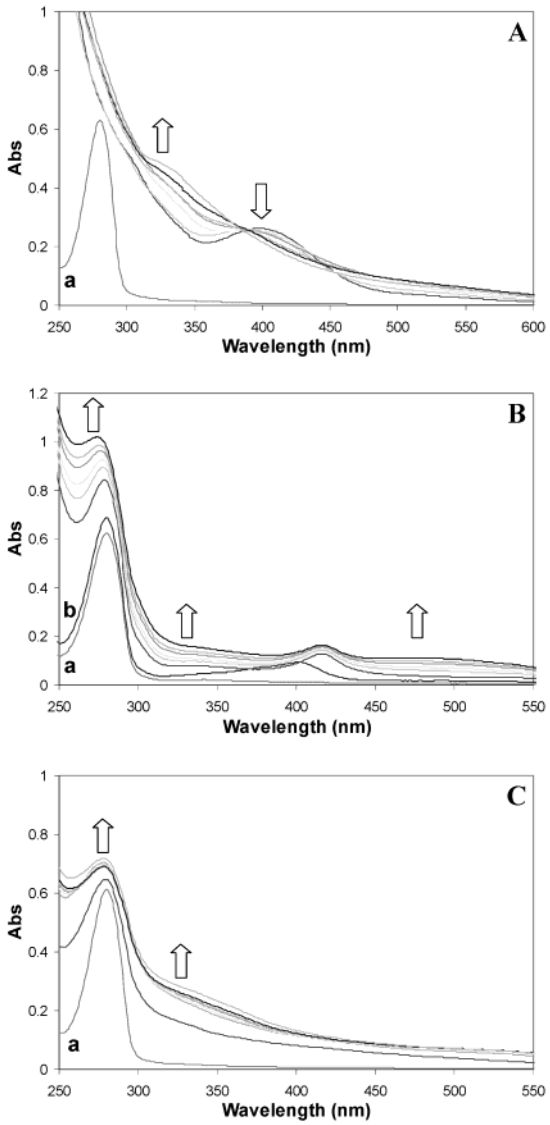

Figure 4. UV−vis spectra for the oxidation of 0.7 mg/mL of **I** ([DOPA] = 0.20 mM) in 10 mM PBS at pH 7.4, with 0.40 mM of $NaIO_4$ (A), 10 units/mL of HRP and 36 mM H_2O_2 (B), and 10 kunits/mL of MT (C). The arrows indicate the progression of the spectra with time. The spectrum of unoxidized **I** is labeled a. In (B), the spectrum of unoxidized **I** with HRP is labeled b, which was obtained prior to addition of H_2O_2.

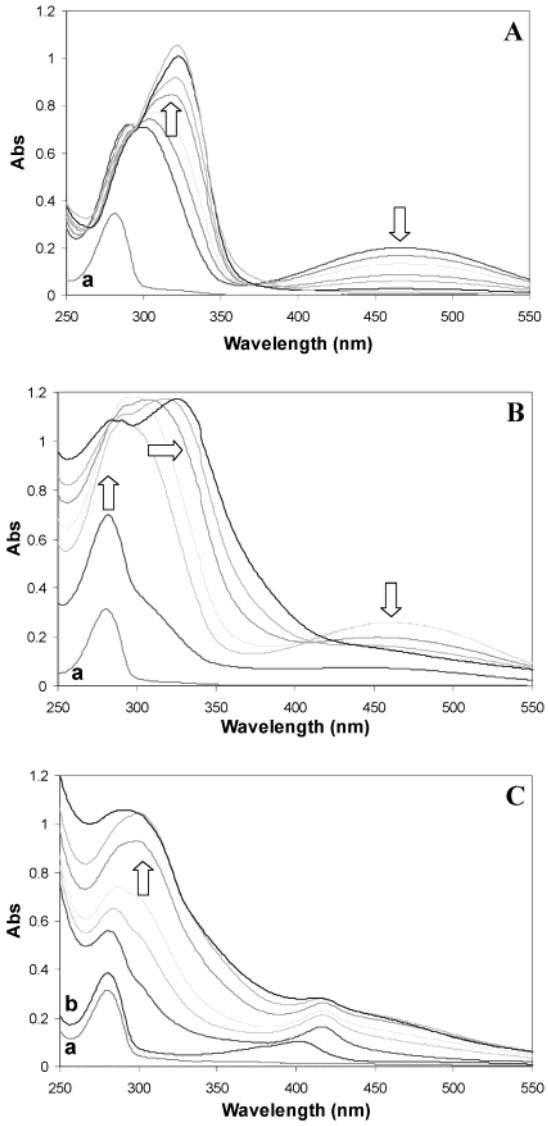

Figure 5. UV−vis spectra for the oxidation of 0.4 mg/mL of **II** ([DOPA] = 0.13 mM) in 10 mM PBS at pH 7.4, with 0.13 mM of $NaIO_4$ (A), 10 kunits/ml of MT/O_2 (B), and 10 units/ml of HRP and 36 mM H_2O_2 (C). The arrows indicate the progression of the spectra with time. The spectrum of unoxidized **II** is labeled a. In (C), the spectrum of unoxidized **II** with HRP is labeled b, which was obtained prior to addition of H_2O_2.

formation and decay of DOPA quinone which was followed by the appearance of characteristic peaks of cyclized DOPA derivatives.[41] These cyclized products as well as the unoxidized catechol are believed to polymerize to form melanin in mammals (Scheme 1, reactions I and J).[42]

Degree of Polymerization and Functionality of the Network Junctions. The observation that solutions of **III** were able to form gels with a high storage modulus (not shown) suggest that DOPA oxidation results in the formation of multifunctional network junctions where more than two DOPA molecules couple together. To determine the functionality of these network junctions, cross-linking reagents were added to aqueous solutions of **IV** and the molecular weights ($\bar{M}_{w,s}^{\mathbf{IV}}$) of the resulting polymers were determined by GPC-MALLS. The RI signal traces of **IV** after 24 h of reaction with several cross-linking reagents are shown in Figure 6. In each case, at least two peaks were detected and their molecular weights were determined. Multimers of **IV** ($\bar{M}_{w,s}^{\mathbf{IV}}/\bar{M}_{w,o}^{\mathbf{IV}} \geq 3$) were easily distinguishable from peaks representing monomers and dimers. In the case of $NaIO_4$-mediated cross-linking, the relative intensities of the multimer and monomer peaks were highly dependent on the $NaIO_4$:DOPA molar ratio (Figure 6A). The maximum conversion of monomer to multimers occurred at roughly equimolar amounts of periodate and DOPA, with the multimer weight fraction (w_s) equal to 0.51. In HRP-induced cross-linking (Figure 6B), the amount of multimers increased with increasing enzyme concentration and w_s varied between 0.33 and 0.67. In MT-mediated reactions (Figure 6C), the amount of multimers formed appeared to be independent to the concentration of MT, with w_s greater than 0.83 at the MT concentrations tested.

The average degree of polymerization of the multimers ($\overline{DP} = \bar{M}_{w,s}^{\mathbf{IV}}/\bar{M}_{w,o}^{\mathbf{IV}}$) was calculated and its dependence on

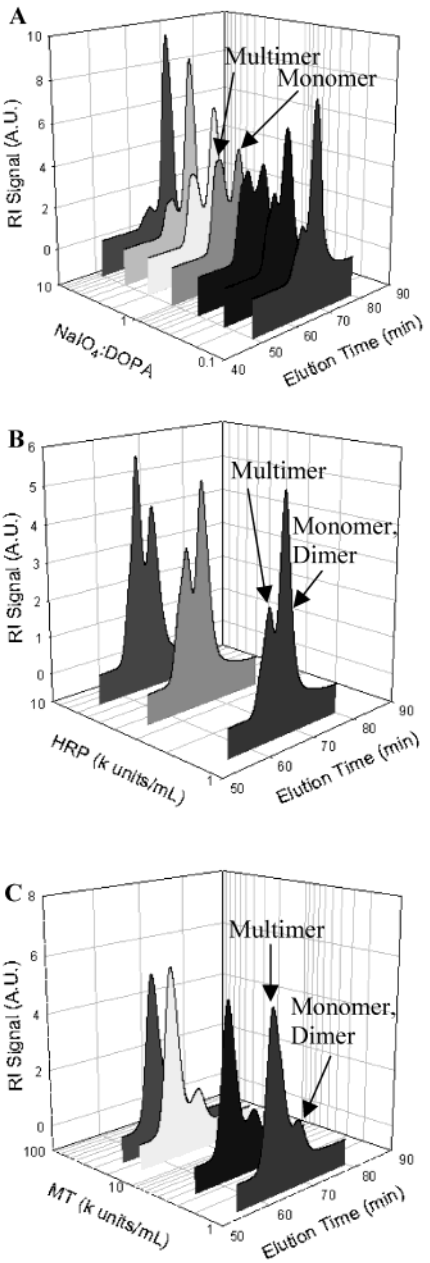

Figure 6. GPC traces of **IV** in 50 mM PBS, 0.1 M NaCl, pH 6.0, 24 h after the initiation of DOPA cross-linking: (A) 10 mg/mL of **IV** and $NaIO_4$; (B) 130 mg/mL of **IV**, HRP, and 0.24 mM of H_2O_2; (C) 130 mg/mL of **IV** and MT. In (B) and (C), **IV** was diluted to 10 mg/mL before analysis.

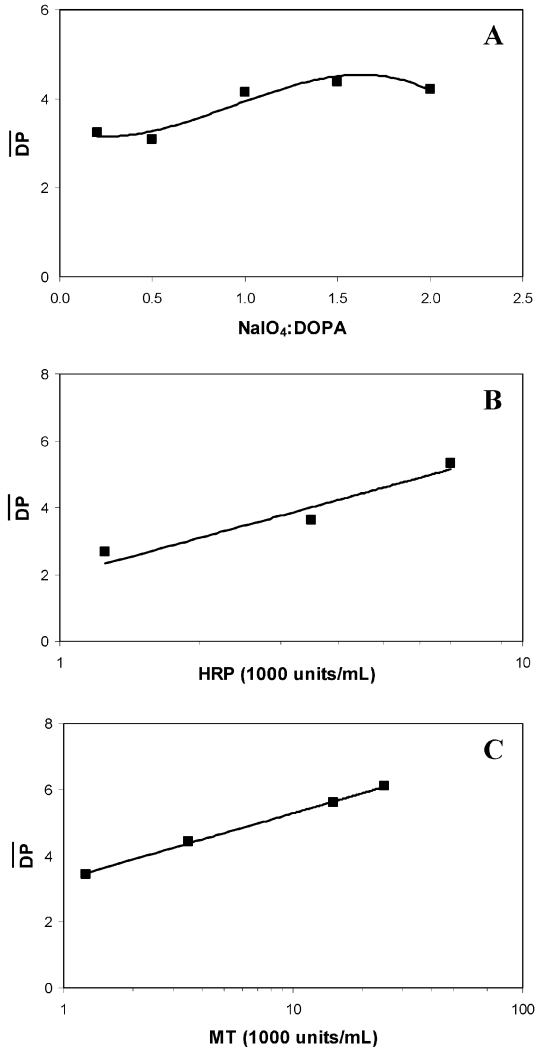

Figure 7. Average degree of polymerization ($\overline{DP}$) of multimers of **IV** (130 mg/mL) determined using GPC-MALLS. **IV** was cross-linked using (A) $NaIO_4$, (B) HRP and 0.24 mM H_2O_2, and (C) MT/O_2 as the oxidizing reagent.

the oxidizing reagent concentration is plotted in Figure 7. For periodate-induced cross-linking (Figure 7A), $\overline{DP}$ varied between 3.0 and 4.5, with the maximum $\overline{DP}$ occurring at $NaIO_4$:DOPA $\approx$ 1.5. In enzymatic-mediated cross-linking (Figure 7B,C), $\overline{DP}$ increased logarithmically with increasing enzyme concentration. The maximum $\overline{DP}$ was 5.2 and 6.4 for HRP and MT-mediated cross-linking, respectively, at the highest enzyme concentrations tested.

When these results are compared with the gelation time experiment (Figure 3), it is clear that the reaction conditions that contributed to extensive multimer formation also contributed to rapid gel formation. For example, using periodate as the cross-linking reagent, at approximately equimolar $NaIO_4$:DOPA, $\overline{DP}$ was greater than 4 and the value of w_s was the greatest. Thus, under these conditions, both high network functionality and conversion contributed to rapid gelation. For HRP-induced cross-linking of **IV**, both $\overline{DP}$ and w_s increased logarithmically while gelation time decreased exponentially with increasing HRP concentration.

The results from the molecular weight analysis indicate that DOPA residues are capable of polymerization to form network junctions consisting of as many as six residues coupled together. The formation of an elastic gel from bifunctional **III** provides strong evidence for this; **III** would form only linear polymers if each DOPA endgroup reacted with just one other DOPA. Although our spectroscopic data confirm the formation of intermediates present during the early stages of the cross-linking reactions (Scheme 1), the intermediates present in the latter stages of the reactions leading to the formation of multifunctional cross-links remain unidentified.

Molecular Weight between Cross-Links. The number average molecular weight between cross-links ($\bar{M}_c$) was determined based on the equilibrium swelling data using eq 3. The average functionality of the network junctions, ϕ, was

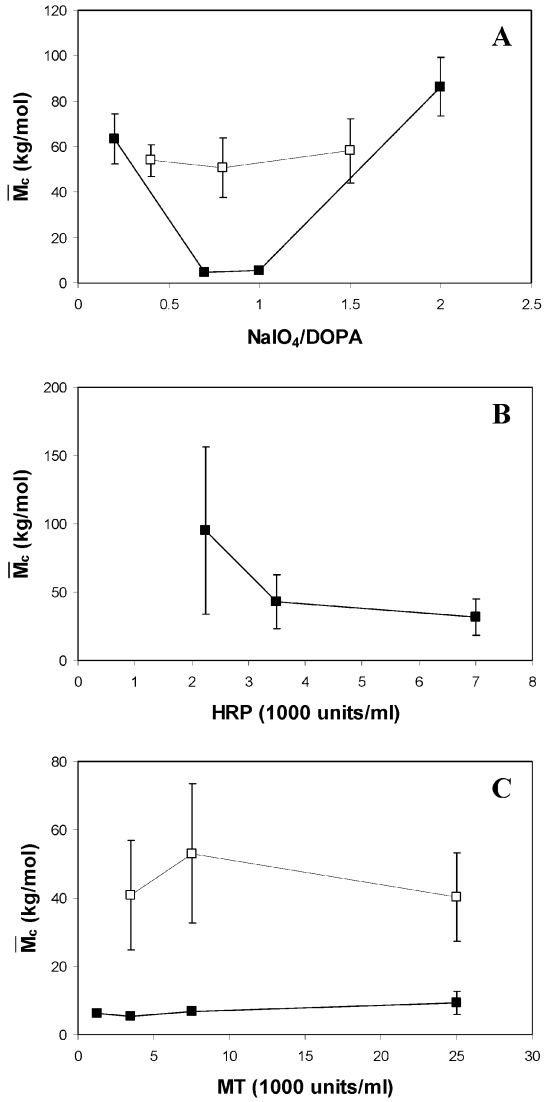

Figure 8. Average molecular weight between cross-link ($\bar{M}_c$) of hydrogels formed from 130 mg/mL solutions of **I** (■) and **III** (□). Oxidizing reagents used were (A) $NaIO_4$, (B) HRP and 0.24 mM H_2O_2, and (C) MT/O_2.

estimated as described above by experimentally determining the degree of polymerization of **IV** using GPC-MALLS under the identical conditions used during gelation of **I** and **III**. The reactivity of DOPA in both **I** and **III** was assumed to be the same as that of **IV**.

The calculated $\bar{M}_c$ values are shown in Figure 8 as a function of cross-linking reagent concentration. From Figure 8A, $NaIO_4$-cross-linked **I** exhibited a minimum $\bar{M}_c$ around 6000 g/mol at $NaIO_4$:DOPA between 0.68 and 1. For PEG-DOPA **III**, $\bar{M}_c$ appeared to be independent of periodate concentration at $NaIO_4$:DOPA between 0.38 and 1.5 ($\bar{M}_c$ values between 50 000 and 60 000 g/mol). Outside of this range, hydrogels of **III** were too fragile to handle, suggesting large $\bar{M}_c$ values. $\bar{M}_c$ for hydrogels formed from HRP/H_2O_2 decreased with increasing HRP concentration as seen in Figure 8B. Gels made from **III** were too fragile to perform swelling experiments, signifying large $\bar{M}_c$. In contrast, $\bar{M}_c$ values for MT/O_2-induced gels (Figure 8C) averaged around 8000 g/mol for **I** and 45 000 g/mol for **III** and did not vary with the concentration of the cross-linking reagent.

Clearly, the architecture of the PEG strongly influenced $\bar{M}_c$. In all three cross-linking reagents utilized, $\bar{M}_c$ was smaller for the branched PEG when compared to its linear counterpart. Assuming that each DOPA endgroup is capable of reacting with at least two others to form a network junction point, the minimum $\bar{M}_c$ values possible for **I** and **III** are 3000 and 4600 g/mol, respectively. In the PEG-DOPA hydrogels, w_s is closely related to the cross-linking density of the gel. In a perfect network, the molecular weight between two consecutive junctions is related to the density of cross-links by[43]

$$M_c = \rho/\upsilon_e \tag{7}$$

where ρ is the density of the network and υ_e is the effective cross-linking density. Although PEG-DOPA hydrogels formed here were not necessarily without defects in the network, a similar inverse relationship between cross-link density and $\bar{M}_c$ was observed.

Molecular weight between cross-links is an important property of a hydrogel that is intimately related to physical properties of the gels.[44,45] For example, swelling and diffusivity, two properties of hydrogels relevant to drug delivery applications, decrease as $\bar{M}_c$ decreases. Furthermore, cross-linking density affects the mechanical properties of the gel and the control of the degree of cross-linking can result in hydrogels with desired mechanical properties.[45] By changing the chemical structure of the PEG backbone and the concentration of the cross-linking reagent utilized, hydrogels with desired physical properties can be achieved.

The DOPA-modified PEGs described here are capable of forming gels through chemically or enzymatically induced cross-linking of DOPA residues. In this method, DOPA residues are incorporated into the gel network and this system can potentially function as a bioadhesive for medical purposes. Although the most rapid gelation was observed through the use of $NaIO_4$, enzymatic approaches may be preferred for medical applications. Residual $NaIO_4$ has the potential to react indiscriminately with surrounding tissues and thus its usage in vivo would have to be preceded by a thorough evaluation of the presence and biological effects of $NaIO_4$ and its reduced forms in the cross-linked gels. Regarding the enzymatically cross-linked gels, it is likely that the HRP and MT enzymes become entrapped within the gel network during cross-linking, either by physical entrapment or by chemical coupling with the reactive oxidized DOPA species. To minimize the adverse biological effects of entrapped enzyme, human-derived peroxidase enzymes found in gastrointestinal tissues[46] and saliva,[47] or the tyrosinase enzymes present in mammalian skin, hair follicle, and retina,[48] can be used instead of HRP and MT.

Conclusion

PEG-DOPA macromers were synthesized using standard peptide chemistry and investigated for their ability to form hydrogels upon addition of oxidizing reagents such as $NaIO_4$, HRP/H_2O_2, and MT/O_2. The gelation time of the DOPA-modified polymers was dependent on the architecture of PEG, the presence or absence of N-terminal protecting

groups, and the type and concentrations of the oxidizing reagents utilized. On the basis of the observed reaction intermediates, possible cross-linking mechanisms for oxidized DOPA residue were proposed. Oxidation of *N*-Boc-protected PEG-DOPA led to cross-linking via phenol coupling and quinone methide tanning, whereas oxidation of deprotected PEG-DOPA led to coupling mechanisms that resembled mammalian melanogenesis. Molecular weight analysis of monosubstituted PEG-DOPA revealed that up to six DOPA molecules react with one another to form a network junction, and rapid gelation was observed under conditions which favored the formation of such junctions. The average molecular weight between cross-links was minimized under these conditions. The results described here indicate that PEG conjugated with DOPA is capable of rapid hydrogel formation. By controlling the chemical structure of the DOPA, the PEG backbone, and the cross-linking reagent concentration, hydrogels with desired $\bar{M}_c$ can be formulated. The adhesive characteristics of these gels are currently being evaluated and will be reported separately.

Acknowledgment. This research was supported by NIH DE13030, DE14193, and T32 DE07042. The authors thank Professor Wesley Burghardt for assistance with rheological measurements.

References and Notes

(1) Waite, J. H. *Int. J. Adhes. Adhes.* **1987**, *7*, 9−14.
(2) Waite, J. H.; Tanzer, M. L. *Biochem. Biophys. Res. Commun.* **1980**, *96*, 1554−1561.
(3) Akemi Ooka, A.; Garrell, R. L. *Biopolymers* **2000**, *57*, 92−102.
(4) Yu, M.; Hwang, J.; Deming, T. J. *J. Am. Chem. Soc.* **1999**, *121*, 5825−5826.
(5) Waite, J. H. *Methods Enzymol.* **1995**, *258*, 1−20.
(6) Waite, J. H. *Ann. N. Y. Acad. Sci.* **1999**, *875*, 301−309.
(7) Ohkawa, K.; Fujii, K.; Nishida, A.; Yamauchi, T.; Ishibashi, H.; Yamamoto, H. *Biomacromolecules* **2001**, *2*, 773−779.
(8) Taylor, S. W.; Chase, D. B.; Emptage, M. H.; Nelson, M. J.; Waite, J. H. *Inorg. Chem.* **1996**, *35*, 7572−7577.
(9) Yamamoto, H. *J. Adhes. Sci. Technol.* **1987**, *1*, 177−183.
(10) Yamamoto, H. *J. Chem. Soc., Perkin Trans. 1* **1987**, 613−618.
(11) Yamamoto, H.; Yamauchi, S.; Ohara, S. *Biomimetics* **1992**, *1*, 219−238.
(12) Yamamoto, H. *Biotechnol. Genet. Eng. Rev.* **1996**, *13*, 133−165.
(13) Berenbaum, M. B.; Williams, J. I.; Bhattacharjee, H. R.; Goldberg, I.; Swerdloff, M. D.; Salerno, A. J.; Unger, P. D. *Polym. Prepr.* **1989**, *30*, 350−351.
(14) Swerdloff, M. D.; Anderson, S. B.; Sedgwick, R. D.; Gabriel, M. K.; Brambilla, R. J.; Hindenlang, D. M.; Williams, J. I. *Int. J. Pept. Protein Res.* **1989**, *33*, 318−327.
(15) Yu, M.; Deming, T. J. *Macromolecules* **1998**, *31*, 4739−4745.
(16) Yamada, K.; Chen, T.; Kumar, G.; Vesnovsky, O.; Topoleski, L. D. T.; Payne, G. F. *Biomacromolecules* **2000**, *1*, 252−258.
(17) Huang, K.; Lee, B. P.; Ingram, D.; Messersmith, P. B. *Biomacromolecules* **2002**, *3*, 397−406.
(18) Huang, K.; Lee, B. P.; Ingram, D.; Messersmith, P. B. *Polym. Prepr.* **2001**, *42*, 147−148.
(19) Lee, B. P.; Dalsin, J. L.; Messersmith, P. B. *Polym. Prepr.* **2001**, *42*, 151−152.
(20) Waite, J. H.; Benedict, C. V. *Methods Enzymol.* **1984**, *107*, 397−413.
(21) Merrill, E. W.; Dennison, K. A.; Sung, C. *Biomaterials* **1993**, *14*, 1117−1126.
(22) Hidalgo, M.; Gonzalez, L.; Mijangos, C. *J. Am. Chem. Soc.* **1996**, *61*, 1251−1257.
(23) Spegt, P. A.; Terrisse, J.; Gilg, B.; Skoulios, A. *Makromol. Chem.* **1967**, *104*, 212−229.
(24) Andreopoulos, F. M.; Beckman, E. J.; Russell, A. J. *Biomaterials* **1998**, *19*, 1343−1352.
(25) Mark, J. E. *Pure Appl. Chem.* **1981**, *53*, 1495−1503.
(26) Sen, M.; Guven, O. *Polymer* **1998**, *39*, 1165−1172.
(27) Gnanou, Y.; Hild, G.; Rempp, P. *Macromolecules* **1984**, *17*, 945−952.
(28) Graham, D. G.; Jeffs, P. W. *J. Biol. Chem.* **1977**, *252*, 5729−5734.
(29) Rzepecki, L. M.; Nagafuchi, T.; Waite, J. H. *Arch. Biochem. Biophys.* **1991**, *285*, 17−26.
(30) Benigni, J. D.; Mnnis, R. L. *J. Heterocycl. Chem.* **1965**, *2*, 387−392.
(31) Sugumaran, M. *Adv. Insect Phys.* **1998**, *27*, 230−334.
(32) Waite, J. H. *Comp. Biochem. Physiol., Part B*: *Biochem. Mol. Biol.* **1990**, *97*, 19−29.
(33) Rzepecki, L. M.; Waite, J. H. *Arch. Biochem. Biophys.* **1991**, *285*, 27−36.
(34) Andersen, S. O.; Jacobsen, J. P.; Roepstorff, P. *Tetrahedron* **1980**, *36*, 3249−3252.
(35) Andersen, S. O.; Roepstorff, P. *Insect Biochem.* **1981**, *11*, 25−31.
(36) Wagner, H. U.; Gompper, R. *Chem. Quinonoid Compd.* **1974**, *Pt. 2*, 1145−1178.
(37) Smith, A. T.; Santama, N.; Dacey, S.; Edwards, M.; Bray, R. C.; Thorneley, R. N.; Burke, J. F. *J. Biol. Chem.* **1990**, *265*, 13335−13343.
(38) Andersen, S. O.; Jacobsen, J. P.; Bojesen, G.; Roepstorff, P. *Biochim. Biophys. Acta* **1992**, *1118*, 134−138.
(39) Waite, J. H.; Tanzer, M. L. *Science* **1981**, *212*, 1038−1040.
(40) McDowell, L. M.; Burzio, L. A.; Waite, J. H.; Schaefer, J. *J. Biol. Chem.* **1999**, *274*, 20293−20295.
(41) Rodriguez-Lopez, J. N.; Tudela, J.; Varon, R.; Garcia-Canovas, F. *Biochim. Biophys. Acta* **1991**, *1076*, 379−386.
(42) Mason, H. S. *J. Biol. Chem.* **1948**, *172*, 83−99.
(43) Barcellos, I. O.; Pires, A. T. N.; Katime, I. *Polym. Int.* **2000**, *49*, 825−830.
(44) Anseth, K. S.; Bowman, C. N.; Brannon-Peppas, L. *Biomaterials* **1996**, *17*, 1647−1657.
(45) Peppas, N. A.; Bures, P.; Leobandung, W.; Ichikawa, H. *Eur. J. Pharm. Biopharm.* **2000**, *50*, 27−46.
(46) Komatsu, H.; Okayasu, I.; Mitomi, H.; Imai, H.; Nakagawa, Y.; Obata, F. *J. Histochem. Cytochem.* **2001**, *49*, 759−766.
(47) Ortiz, G. C.; Rahemtulla, B.; Tsurudome, S. A.; Chaves, E.; Rahemtulla, F. *Eur. J. Oral Sci.* **1997**, *105*, 143−152.
(48) Riley, P. A. *Int. J. Biochem. Cell Biol.* **1997**, *29*, 1235−1239.

BM025546N